

## Mechanism for the Formation of PNIPAM/PS Core/Shell Particles

Li Zhang,<sup>1,2</sup> Eric S. Daniels,<sup>1</sup> Victoria L. Dimonie,<sup>1</sup> Andrew Klein<sup>1,3</sup>

<sup>1</sup>Emulsion Polymers Institute, Lehigh University, Bethlehem, Pennsylvania 18015

<sup>2</sup>Department of Chemistry, Lehigh University, Bethlehem, Pennsylvania 18015

<sup>3</sup>Department of Chemical Engineering, Lehigh University, Bethlehem, Pennsylvania 18015

Correspondence to: E. S. Daniels (E-mail: Eric.Daniels@Lehigh.edu)

**ABSTRACT:** A multi-stage polymerization method was previously used to prepare PNIPAM/PS core/shell particles that exhibited uniform “raspberry-like” structures. In this current study, this polymerization process was carefully investigated in order to elucidate the PS (polystyrene) shell formation mechanism. The results indicated that the “raspberry” structure is due to heterocoagulation of polystyrene domains onto PNIPAM (poly(*N*-isopropylacrylamide)) particle surfaces. Different sizes and numbers of the PS domains can be obtained by varying the styrene feed rate. It was also found that linear PNIPAM may increase the compatibility between PNIPAM and PS polymers. In addition, this heterocoagulation mechanism for forming structured particles was successfully applied to a PNIPAM and Ludox<sup>®</sup> colloidal silica nanoparticle system where a core/shell structure was also obtained. © 2013 Wiley Periodicals, Inc. *J. Appl. Polym. Sci.* **2014**, *131*, 40124.

**KEYWORDS:** colloids; emulsion polymerization; gels; lattices; morphology

Received 15 August 2013; accepted 26 October 2013

DOI: 10.1002/app.40124

### INTRODUCTION

In recent years, a great deal of interest has been focused on thermosensitive polymers due to their fast reversible structural change that occurs at a specific temperature, termed the lower critical solution temperature (LCST). For thermosensitive polymer microspheres, this transition is reflected by a large volume change; hence, this temperature is called the volume phase transition temperature (VPTT). Among all of the thermosensitive polymers, poly(*N*-isopropylacrylamide) (PNIPAM) is the best known and studied polymer with a LCST  $\sim 31\text{--}32^\circ\text{C}$ .<sup>1</sup>

In our previous paper,<sup>2</sup> two different polymerization methods were used to prepare PNIPAM/PS core/shell particles, either above or below the volume phase transition temperature (VPPT) using either a multi-stage or semi-batch polymerization process. In both processes, uniform “raspberry” structures were obtained in which polystyrene formed small domains on the surface of the PNIPAM particles. The resulting core-shell structure was confirmed by temperature-dependent particle size and density gradient experiments. This type of particle may potentially be applied to areas such as bio-diagnostic applications,<sup>3,4</sup> bioseparation,<sup>5</sup> drug delivery,<sup>6</sup> catalysts,<sup>7</sup> and pollution control.<sup>8</sup> Therefore, it is of great importance to understand the mechanism of PNIPAM/PS core-shell particle formation.

There are a several reports in the literature which showed that a “raspberry” structure was obtained while using NIPAM as one

of the monomers. For example, Duracher et al.<sup>5</sup> tried to synthesize NIPAM-styrene copolymer latex containing amino groups in the shell using a two-step emulsifier-free polymerization process. It was found that the raspberry-like structure was more obvious when the amino group-containing monomer was added at lower conversions. The authors explained that the “raspberry” structure was the result of phase separation because of poor compatibility between the two polymers. Zhou et al. introduced a cyano functional group into the PNIPAM particles by using an emulsifier-free two-step polymerization process.<sup>9</sup> “Raspberry” structured particles were also obtained in this case. The author indicated that both phase separation and heterocoagulation may be the reasons for obtaining “raspberry” structured particles. However, during the reaction, small particles were never observed by QELS, which did not confirm the heterocoagulation mechanism.

In this present study, in order to elucidate the PS shell formation mechanism, samples were taken during the polymerization and carefully characterized. The results indicated that the “raspberry” structure is due to heterocoagulation. By varying the feeding rate, the obtained “raspberry” structured particles exhibit different domain sizes and domain numbers, which also supports the hypothesis that polystyrene particles were first generated in the aqueous phase and then heterocoagulated with PNIPAM microspheres. This view is further strengthened by the observed “raspberry” structured particles that were obtained by

employing a simple mixing experiment with PS and PNIPAM particles. It was also found that linear PNIPAM may increase compatibility between PNIPAM and PS. In addition, this heterocoagulation mechanism of forming core/shell structured particles was successfully applied to a PNIPAM and Ludox<sup>®</sup> colloidal silica nanoparticle system. The resulting core/shell particles have PNIPAM as the core and Ludox<sup>®</sup> colloidal silica nanoparticles as a shell layer. This core/shell heterocoagulation formation method may open up a number of opportunities in forming structured microspheres.

## EXPERIMENTAL

### Materials

*N*-isopropylacrylamide (NIPAM; 99%, VWR International) was recrystallized from mixtures of toluene and hexane (in a volume ratio of 2:3). *N,N'*-methylenebisacrylamide (MbAA; 99%, Fisher Scientific), potassium persulfate (KPS; Fisher Scientific), L-ascorbic Acid (99%, Sigma–Aldrich), hydrogen peroxide, (H<sub>2</sub>O<sub>2</sub>; 35%, Sigma–Aldrich), ferrous sulfate (FeSO<sub>4</sub>·7H<sub>2</sub>O; Fisher Scientific), and sodium dodecyl sulfate (SDS; Sigma–Aldrich) were all used as received. Ludox<sup>®</sup> colloidal silica was used as received (VWR, HS-30 colloidal silica, 30 wt % suspension in water). Deionized (DI) water was used in all experiments.

### Synthesis of Poly(*N*-isopropylacrylamide) Core and Polystyrene Shell Synthesis using a Multistage Process at 70°C

The detailed description of the procedure used to prepare PNIPAM particles and PNIPAM/PS core/shell particles was shown previously.<sup>2</sup>

### Determination of Instantaneous Conversion of Styrene during the Shell Formation Stage

The instantaneous conversion of styrene (St) was monitored during the shell formation reaction. Samples were taken at 15, 30, 45, 60, 120, 180 min, and at the end of the polymerization. The amount of unreacted monomer was determined by gas chromatography (Hewlett Packard 5890) with dioxane as an internal standard. The instantaneous styrene conversion is calculated as:

$$\text{Instantaneous Conversion (\%)} = \left[ 1 - \frac{\text{unreacted styrene (wt.)}}{\text{styrene fed (wt.)}} \right] \times 100\% \quad (1)$$

**Determination of Particle Size.** The particle diameter and size distributions of the latex particles were measured by dynamic light scattering (Nicomp, Model 370) at 25°C and by capillary hydrodynamic fractionation at 35°C (CHDF 1100 and 2000, Matec Applied Sciences). They were also measured (in a dry state) by transmission electron microscopy (TEM, Philips 400T), measuring 600 particles for each sample.

### Determination of Linear Polymer Fraction in PNIPAM

Ultracentrifugation was used to separate the linear PNIPAM fraction from the crosslinked PNIPAM fraction. The samples were ultracentrifuged (Beckman Coulter, Optima L-90K) at 30,000 rpm at 5°C for 2 h. The soluble linear PNIPAM was present in the top layer of the centrifuge tube, while crosslinked PNIPAM that was swollen with a small amount of water was present at the bot-

**Table I.** Dilution of the Solution for Viscosity Measurement at 24.5°C

Concentration of aqueous PNIPAM solution	Initial solution	1st Dilution	2nd Dilution	3rd Dilution	4th Dilution
C (g mL <sup>-1</sup> )	0.0134	0.0094	0.0072	0.0049	0.0037

tom of the tube. By drying the samples obtained from the top layer and the bottom layer of the centrifuge tube, the solids contents of the two layers could be obtained through gravimetric analysis. Because the original PNIPAM latex solids content is known, the linear fraction of PNIPAM can be calculated.

### Measurement of Interfacial Tension using the Drop Volume Method

The interfacial tension between styrene and various concentrations of aqueous linear PNIPAM solution were determined by drop volume measurements. Linear PNIPAM was synthesized separately using a redox initiator system at room temperature. No surfactant was added during the reaction. The aqueous linear PNIPAM solutions prepared at various concentrations were slowly metered into styrene with a syringe pump at various rates (0.13, 0.14, 0.18, 0.33, 0.5, 0.6 mL min<sup>-1</sup>) through a capillary (diameter = 1.03 mm), forming drops at 6 and at 28°C, respectively. When the droplet detached, the volume of each drop and the corresponding time were recorded. By using the method developed by Lando and Oakley,<sup>10</sup> the interfacial tensions could be calculated.

**Viscosity Measurements.** An Ubbelohde viscometer (Cannon, D674, 100 mL) was used to measure the efflux time of the linear PNIPAM solution. Different concentrations of solutions were prepared according to Table I. The solvent used was water. The relative viscosity,  $\eta_r$ , the specific viscosity,  $\eta_{sp}$ , and the reduced viscosity  $\eta_{red}$  were calculated according to eqs. (2–4).

$$\eta_r = \frac{\eta}{\eta_0} \approx \frac{t}{t_0} \quad (2)$$

$$\eta_{sp} = \eta_r - 1 \quad (3)$$

$$\eta_{red} = \frac{\eta_{sp}}{c} \quad (4)$$

In the equations,  $t$  is the efflux time for each solution and  $t_0$  is the efflux time for the solvent (H<sub>2</sub>O in this case).

### Cleaning of Latex

The latex was cleaned by the serum replacement process.<sup>11</sup> After diluting the latex to 5% solids content in water, the latex was fitted with a 200 nm pore size membrane (GE Water & Process Technologies). The latex was cleaned by passing 30–40 residence volumes (400 mL) of DI water through the latex. The serum replacement process was continued until the conductivity of the serum was close to that of deionized water (0.35  $\mu\Omega$  cm<sup>-1</sup>).

## RESULTS AND DISCUSSION

### Shell Formation Mechanism Study

To understand the mechanism of the formation of “raspberry” structured particles, samples were taken during the reaction at

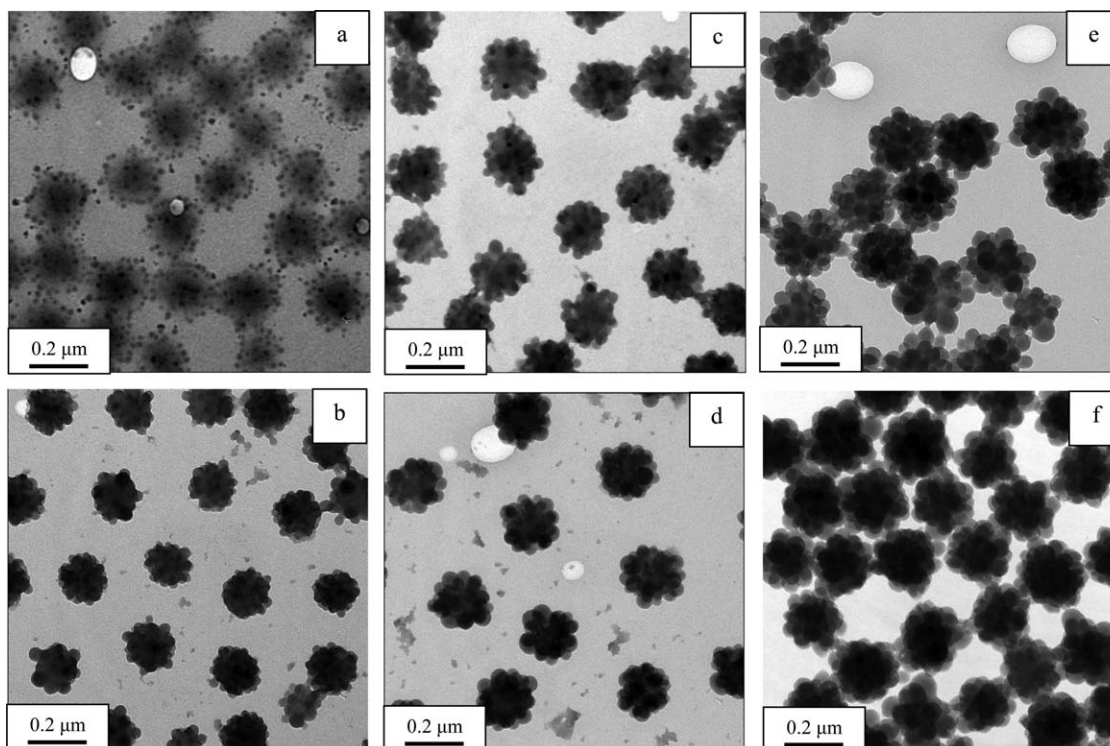


**Figure 1.** Multistage shell formation as a function of the styrene feed time: (a) 15 min,  $\times 25K$ , (b) 45 min,  $\times 25K$ , (c) 1 h,  $\times 25K$ , (d) 2 h,  $\times 25K$ , (e) 3 h,  $\times 25K$ , and (f) end of the reaction,  $\times 25K$ .

15 min, 45 min, 1 h, 2 h, and 3 hr into the feed process, and at the end of the polymerization. TEM micrographs of each sample are shown in Figure 1. At 15 min, small polystyrene particles (PS) were observed which appeared to be attached to the PNIPAM particle surfaces. These small individual polystyrene particles were  $\sim 20$  nm in diameter [Figure 1(a)]. After 45 min of feeding, small domains were observed as hemispheres on the surface of the PNIPAM particles. The domain size increased to about 35 nm [Figure 1(b)]. After 1, 2, and 3 h of styrene feeding, the particle size became larger and the contours of the particles became more obvious. By the end of the reaction, well-defined “raspberry” particles were obtained and the polystyrene domain size reached 65 nm [Figure 1(f)].

From Figure 1, it was shown that at 15 min of polymerization, each of the individual PS particles appeared to be spherical. However, up to 45 min of monomer feed, each PS particle resembled a hemisphere. Therefore, by assuming that each domain was a hemisphere at this time and that the number of PS particles was constant, the theoretical domain size could be calculated and is shown in Figure 2. It was found that in the first hour of polymerization the domain size measured from the TEM micrographs agrees very well with the theoretical domain size. However, after 2 h, the experimental domain size was 10 nm larger than the calculated domain size. This may be explained by the assumption that the domains were hemispheres may be not correct, or the number of PS domains may not remain exactly the same during the feeding process. Therefore, in this experiment, larger PS domains were observed. This experiment also indicates that the polystyrene particles may first

be generated in the aqueous phase and then heterocoagulate onto the surface of the PNIPAM particles, when these PS particles grew to a certain critical size.

The instantaneous conversion of styrene was also monitored during the shell formation reaction. Samples were taken at 15, 30, 45, 60, 120, 180 min, and at the end of the reaction. The amount of unreacted monomer was determined by GC with dioxane as an internal standard. The results are listed in Table II. The instantaneous conversion was quite high, remaining at  $\sim 95\%$ , at which level the  $T_g$  of polystyrene was  $76^\circ\text{C}$  based on

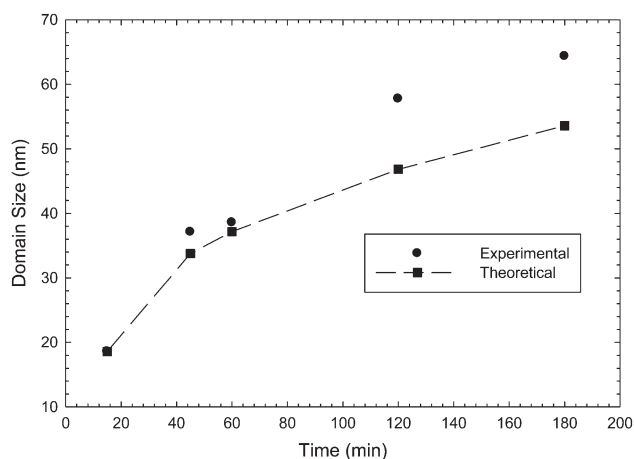


**Figure 2.** Polystyrene domain size as a function of the styrene feeding time.

**Table II.** Styrene Instantaneous Conversion in Multistage Polymerization at 70°C

Feed time (min)	Styrene feed (g)	Conv.
15	0.41	94.6%
30	0.82	95.5%
60	1.64	94.9%
120	3.28	96.4%
180	4.92	96.6%
End	6.55	99.3%

a calculation given by Harris et al.<sup>12</sup> This explains why the domains present on the surface of the particles did not coalesce with each other, but rather maintained their shapes during the reaction. In addition, under these highly monomer-starved feeding conditions, it is difficult to generate additional PS particles after the nucleation stage was complete, which helps to limit the formation of any secondary population of PS homopolymer latex particles. This was also suggested by the uniform small “domain” diameter. The domain size distribution was 1.10, which is narrow considering that the domain size is in the range of 50–60 nm.

To investigate the effect of the feeding rate on the particle morphology, a series of experiments were carried out. The change in the number and diameter of the domains present on the particle surface was correlated with the variation of the styrene feed rate from 15 to 30 to 60  $\mu\text{L min}^{-1}$  at the end of reaction. The corresponding TEM micrographs are shown in Figure 3.

For a feed rate of 60  $\mu\text{L min}^{-1}$ , it was observed that the domain diameter was smaller, and the domain size distribution was broader, compared to that found with a feeding rate of 30  $\mu\text{L min}^{-1}$ . In addition, the number of domains was much larger, and many of them existed as free polystyrene particles. For the 15  $\mu\text{L min}^{-1}$  feeding rate, the polystyrene domain number is smaller and the domain diameter was larger compared with that obtained at 30  $\mu\text{L min}^{-1}$  feeding rate.

The existence of free polystyrene particles may indicate that styrene polymerizes in the aqueous phase first and as the particles grow, they cannot be fully stabilized, and hence, they become coagulated onto the surface of the PNIPAM particles. When the styrene feed rate was too high, too many polystyrene particles were generated, and there was not enough PNIPAM surface area to capture all of the polystyrene particles. Therefore, some individual free polystyrene particles remained in the aqueous phase at the end of the reaction. In addition, the samples taken during the course of the polymerization showed that the polystyrene particles grew on the PNIPAM surfaces, after they coagulated. When the feed rate was low, all of the polystyrene particles generated in the aqueous phase coagulated on the PNIPAM surface. The number of polystyrene particles was lower in this case, and each polystyrene particle had a higher amount of styrene which allowed the particles to grow larger. The experimental evidence clearly favors the view that styrene was polymerized first in the aqueous phase and then subsequently heterocoagulates with PNIPAM particles.

It was found that 11% linear PNIPAM polymer was formed during the seed stage by employing the ultracentrifugation

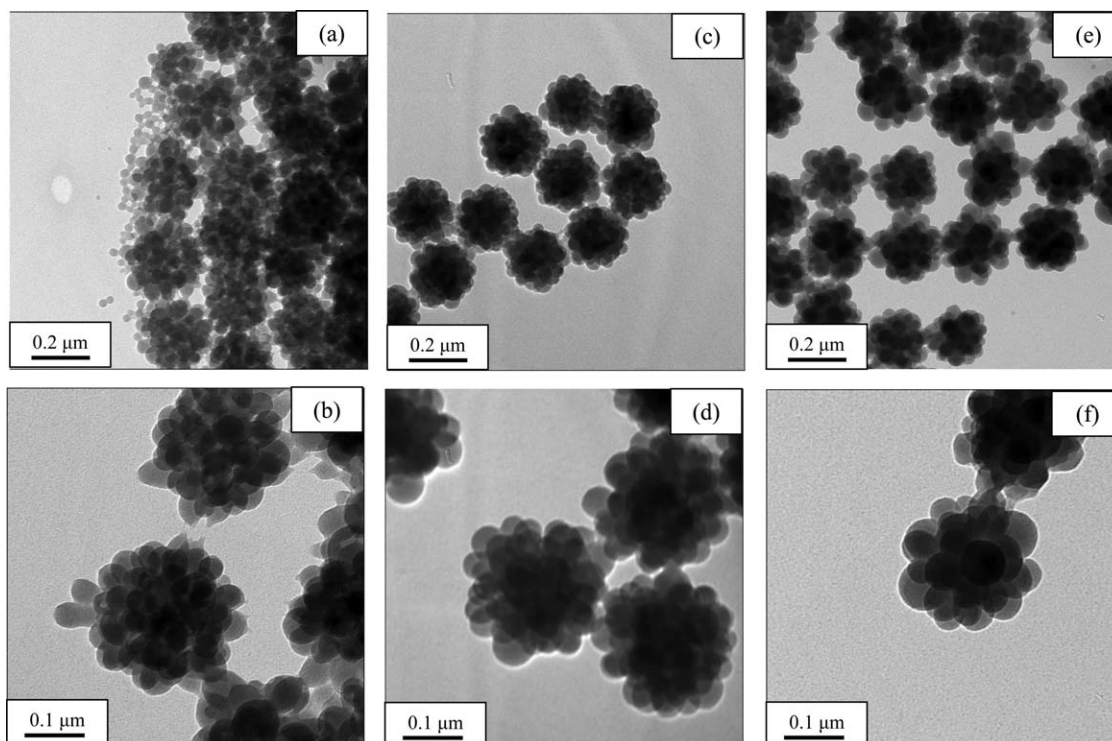


**Figure 3.** Multistage shell formation with the styrene feeding rate at: (a) 60  $\mu\text{L min}^{-1}$ ,  $\times 25\text{K}$  (b) 60  $\mu\text{L min}^{-1}$ ,  $\times 54\text{K}$  (c) 30  $\mu\text{L min}^{-1}$ ,  $\times 25\text{K}$ , and (d) 30  $\mu\text{L min}^{-1}$ ,  $\times 54\text{K}$ ; (e) 15  $\mu\text{L min}^{-1}$ ,  $\times 25\text{K}$ ; (f) 15  $\mu\text{L min}^{-1}$ ,  $\times 54\text{K}$ .

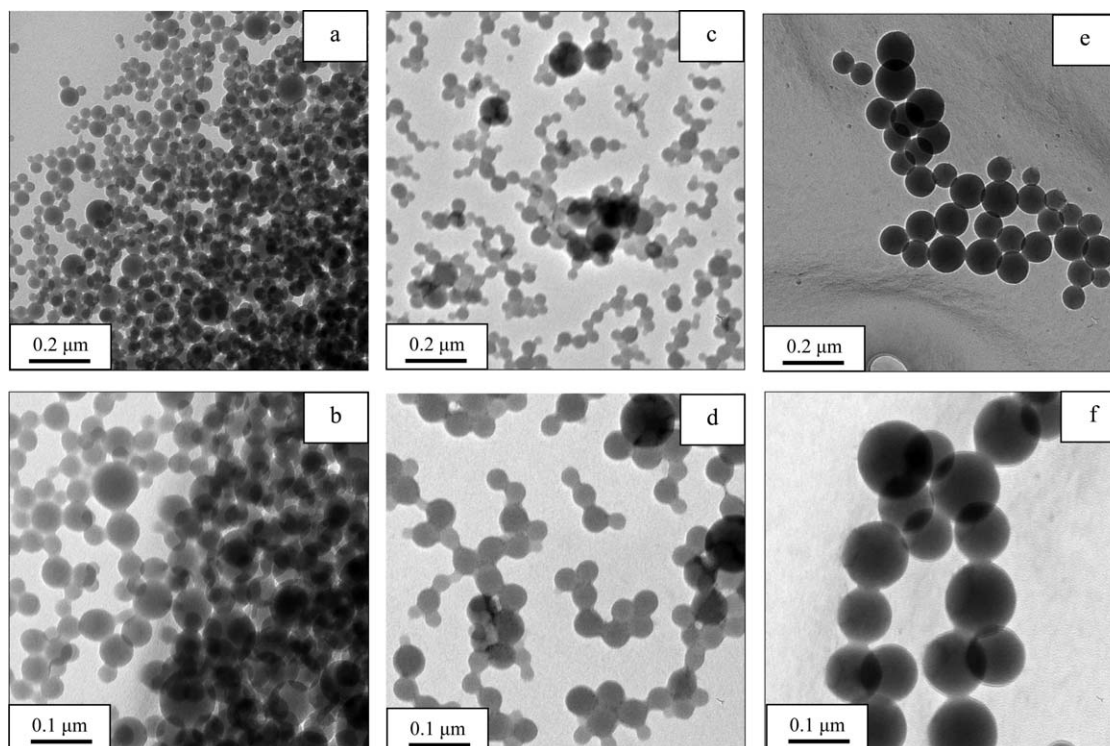


**Figure 4.** Effect of Linear PNIPAM in multistage shell formation experiment with styrene feed rates of (a)  $60 \mu\text{L min}^{-1}$ ,  $\times 25\text{K}$ , (b)  $60 \mu\text{L min}^{-1}$ ,  $\times 54\text{K}$ , (c)  $30 \mu\text{L min}^{-1}$ ,  $\times 25\text{K}$ , (d)  $30 \mu\text{L min}^{-1}$ ,  $\times 54\text{K}$ , (e)  $30 \mu\text{L min}^{-1}$ ,  $\times 25\text{K}$  without L-PNIPAM, (f)  $30 \mu\text{L min}^{-1}$ ,  $\times 54\text{K}$  without L-PNIPAM.

separation method. These linear PNIPAM (L-PNIPAM) polymers generated during the NIPAM polymerization are suspected to help stabilize the small PS particles generated during the multistage shell formation. To investigate this, a series of shell formation experiments were carried out by using the typical shell formation recipe, except that all of the PNIPAM particles were removed from the PNIPAM seed latex by centrifugation and only the serum was used for the reaction; i.e., the continuous phase contained only linear PNIPAM. Two styrene feed rates, 30 and  $60 \mu\text{L min}^{-1}$  (L-PNIPAM\_30 and L-PNIPAM\_60, respectively) were tested. In a control experiment (St\_30), 100 mL water was used instead of the linear PNIPAM serum and the styrene feed rate was  $30 \mu\text{L min}^{-1}$ . The corresponding TEM pictures are shown in Figure 4 and the particle diameter results are shown in Table III. The control experiment, in which no linear PNIPAM was used, produced a particle with a diameter of  $\sim 120 \text{ nm}$  and a particle size distribution of 1.12. In the presence of linear PNIPAM, the size of the polystyrene particles was  $\sim 60 \text{ nm}$  ( $D_w$ ) at  $30 \mu\text{L min}^{-1}$  and  $\sim 70 \text{ nm}$  ( $D_w$ ) at  $60 \mu\text{L min}^{-1}$ . The experiment showed that in the presence of linear PNIPAM, the polystyrene particle size was greatly reduced. The higher feeding rate generated a broader particle diameter distribution.

These experimental findings can be explained as follows. At the beginning of the polymerization reaction, a large number of free PS particles were generated. However, when these particles grew to a certain size, the amount of available surfactant was not sufficient to stabilize all of the particles. Hence, they coagulated or coalesced with one another to reduce the surface area

by forming larger particles as shown in the case of the control experiment. On the other hand, if the PS particles possess a stabilizing barrier layer, such as linear PNIPAM, which can function as a steric stabilizer, smaller polystyrene particles can result. In addition, it is interesting to note that the particle size generated at a styrene feed rate of  $30 \mu\text{L min}^{-1}$  is very close to the domain size of the “raspberry” structured particles. This also supports the hypothesis that polystyrene particles may first be generated in the aqueous phase and then heterocoagulate with PNIPAM particles. It was also observed that the polystyrene particles generated in the presence of linear PNIPAM appeared to be connected with each other. This may be due to the presence of the linear PNIPAM polymers. The same kind of phenomena where particles were connected, was observed in TEM micrographs of uncleaned PNIPAM particles (i.e., having linear PNIPAM remaining on the particle surface).<sup>13</sup> It is not clear whether this is due to the drying process during the TEM sample preparation or if linear PNIPAM polymers had been adsorbed on the polystyrene particle surfaces before the drying process.

**Table III.** Particles Size (TEM) Results Showing the Influence of Linear PNIPAM in Multistage Polymerization

	$D_n$ (nm)	$D_w$ (nm)	$D_v$ (nm)	PDI
L-PNIPAM_60	45.1	73.8	51.2	1.63
L-PNIPAM_30	41.4	61.7	45.2	1.29
St_30	114	127	118	1.12

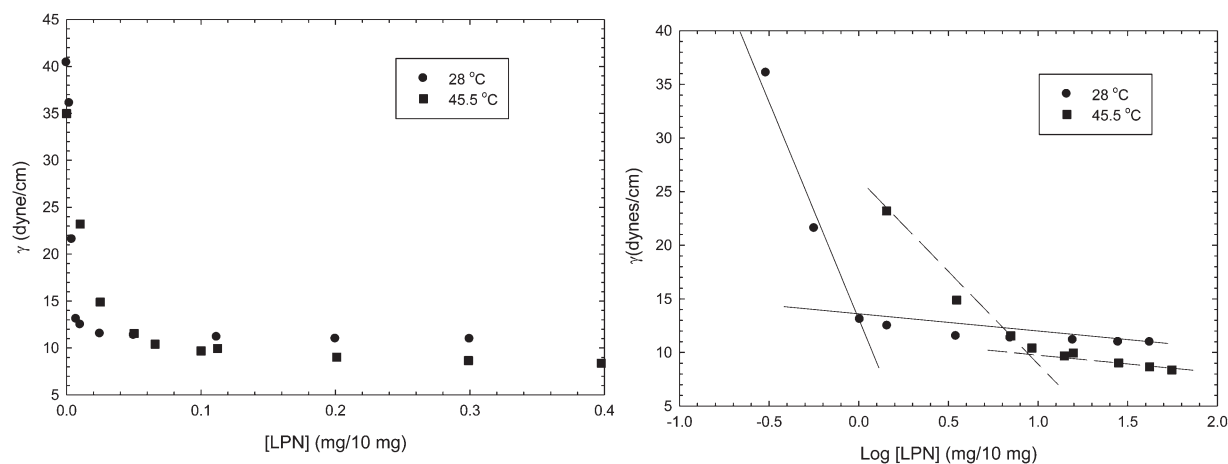


**Figure 5.** Interfacial tensions as a function of (a) [LPN] at 28.0 and 45.5°C and (b) log [LPN] at 28 and 45.5°C.

To further confirm the surface-active properties of linear PNIPAM, drop volume measurements were carried out to determine the interfacial tension between styrene and various concentrations of aqueous linear PNIPAM solution. The results are shown in Figure 5. At 28°C, it was found that the interfacial tension decreased from 40 to 11 dyne  $\text{cm}^{-1}$  as the concentration of linear PNIPAM was increased. When the linear PNIPAM concentration was further increased, the interfacial tension leveled off. At 45.5°C, the same phenomenon was observed, and the interfacial tension dropped from 36 to 13 dyne  $\text{cm}^{-1}$  and then leveled off. If this result is replotted using a log scale as in Figure 5(b), then the typical “elbow” transition point reflecting the CMC for a surfactant can be determined. It is especially apparent at 28.0°C, where the cmc was found to be  $1.02 \times 10^{-2}$  wt %. Zhang and Pelton showed that linear poly(*N*-isopropylacrylamide) was surface active at 25°C.<sup>14</sup> They also showed that at a temperature higher than the LCST, depending on the solution concentration, that two different events may occur. One experimental concentration was 10 mg  $\text{L}^{-1}$ , where PNIPAM did not influence the surface tension above 35°C. On the other hand, for concentrations below 10 g  $\text{L}^{-1}$  PNIPAM exhibited surface activity both at 25 and 40°C. It is possible that linear PNIPAM could form colloidal particles that in a limited way could diffuse to the air/water interface, unfold, and adsorb at this interface to lower the surface tension.<sup>14,15</sup> In our research, most of the tested concentrations of linear PNIPAM were well above 10 mg  $\text{L}^{-1}$ . It was also shown that even above the LCST, linear PNIPAM exhibited surface activity. The reported molecular weight of PNIPAM was  $\sim 8 \times 10^5$  g  $\text{mol}^{-1}$ , which is equivalent to what was used in this research.<sup>14,15</sup> At high temperatures, it was observed that the linear PNIPAM exhibited some surface activity even at 45.5°C. This may occur because the presence of the hydrophobic styrene helps to unfold the PNIPAM collapsed chains, which allows them to function as stabilizers. Furthermore, these results provide evidence that linear PNIPAM functions as a stabilizer for polystyrene particles formed in the aqueous phase.

The viscosity-average molecular weight of the linear PNIPAM synthesized using redox initiator was measured by using dilute

viscosity measurements. The intrinsic viscosity can be measured by experiments based on Huggin’s and Kramer’s equations.<sup>16,17</sup>

$$\frac{[\eta_{\text{sp}}]}{c} = [\eta] + k'[\eta]^2 c \quad (5)$$

$$\frac{\ln [\eta_r]}{c} = [\eta] - k''[\eta]^2 c \quad (6)$$

The obtained results are shown in Figure 6 and Table IV. It is known that at 25°C for PNIPAM dissolved in water, the Mark-Houwink equation can be expressed as the following<sup>18</sup>:

$$[\eta]/(\text{mLg}^{-1}) = 2.26 \times 10^{-1} M^{0.97} \quad (7)$$

Therefore, the viscosity-average molecular weight of linear PNIPAM was calculated to be  $5.63 \times 10^5$  g  $\text{mol}^{-1}$ , which is close to what Zhu et al. obtained.<sup>18</sup>

To test the strength of the interaction between the PS domains and the PNIPAM particles, the “raspberry” structured latex was sonified for 10 or 15 min in the presence of additional surfactant (SDS) (Branson sonifier, duty cycle 60, output setting of 7). The same conditions are normally used for preparing miniemulsions. The results obtained from TEM micrographs (Figure

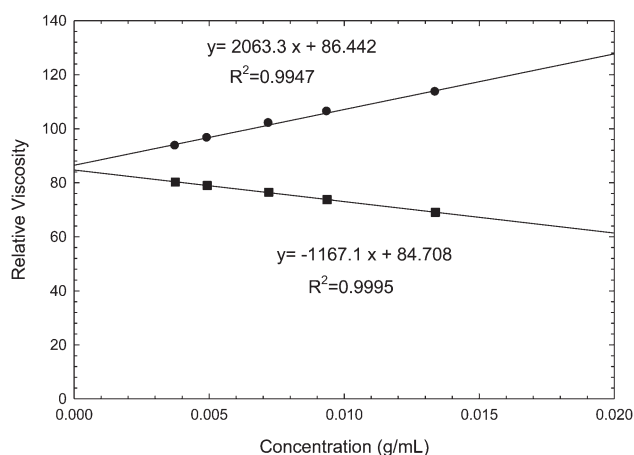


**Figure 6.** Viscosity measurement of linear PNIPAM prepared by using redox polymerization.

**Table IV.** Viscosity-average Molecular Weight of Linear PNIPAM

$[\eta]$	85.575
$K'$	0.28
$K''$	-0.16
$K'-K''$	0.44
$K^{31}$	2.26E-04
$\alpha^{31}$	0.97
$M_v$ (g mL <sup>-1</sup> )	5.63E+05

7) indicated that the particles still maintained their “raspberry” structure. To exclude the possibility of PS particles coagulating with PNIPAM after the sonification is complete, extra surfactant was added to the solution to stabilize any small polystyrene particles that were desorbed off of the PNIPAM surface by sonification. However, as shown in Figure 7(e,f), the particles still possessed the “raspberry” structure. These results indicate that this association between PNIPAM and PS particles was very strong.

The simplest way to further confirm that the PS shell formation results from the heterocoagulation process is to mix PS latex particles with PNIPAM latex particles in various ratios. Therefore, PS latex particles shown in Figure 4 (L-PNIPAM 30) were utilized in the mixing experiment while PNIPAM latex particles were synthesized individually by following the synthesis method described in the literature.<sup>2</sup> The corresponding particle sizes were measured by CHDF as shown in Figure 8. The PS particles have a mean diameter of 65 nm, while the diameter for the

PNIPAM particles was 166 nm. The PNIPAM latex was added dropwise to the PS latex while stirring the solution with a magnetic stir bar at room temperature. The two types of latexes were mixed together at different ratios, and the final latexes were examined by TEM. When the mixing weight ratio of PS/PNIPAM was 5.27, as shown in Figure 9(a,b), it was observed that the PNIPAM particle surface was fully covered by PS particles. However, there were many individual free PS particles present. This may be because the ratio of PS to PNIPAM was too high, and after all of the surfaces of PNIPAM particles were covered by PS particles, there were still extra PS particles that remained in the aqueous phase. When the PS/PNIPAM particle weight ratio was reduced to 2.98 as shown in Figure 9(c,d), the PNIPAM surface coverage was still good and there were less individual PS particles present in the aqueous phase. When the weight ratio was reduced further to 1.97, as shown in Figure 9(e,f), the surface of PNIPAM particles was uniformly covered by PS particles. All of the particles exhibited a “raspberry” structured morphology. In addition, not many individual PS particles were observed. After further reducing the ratio to 1.23 as shown in Figure 9(g,h), two types of particles with different morphologies were observed. One type of particle exhibited a uniform “raspberry” morphology, while the other type of particle exhibited a large area where the particle surface was bare next to a few attached PS particles.

It is also interesting to note that at the weight ratio of 1.23 PS/PNIPAM, some of the PNIPAM particles were fully covered by polystyrene particles, while some of the PNIPAM particles were only covered by a small number of PS particles. This may be

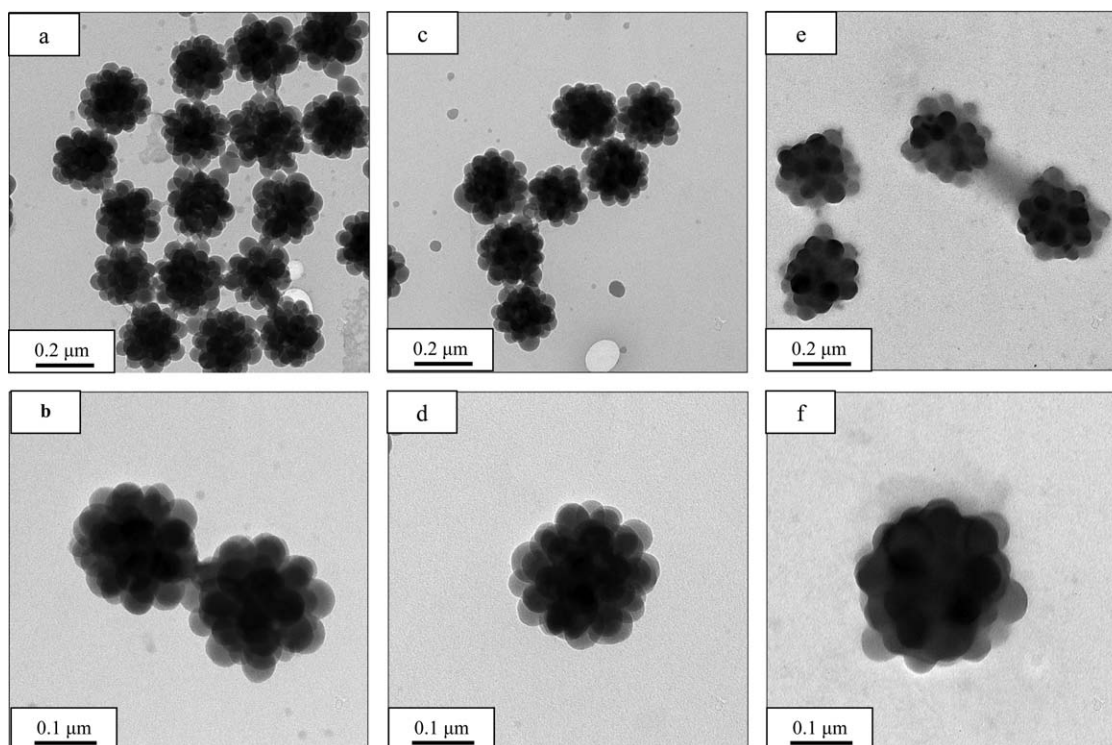


**Figure 7.** TEM micrographs of the “raspberry” structured particles after sonification for: (a) 10 min,  $\times 25K$ , (b) 10 min,  $\times 54K$ , (c) 15 min,  $\times 25K$ , (d) 15 min,  $\times 54K$  (e) 10 min,  $\times 25K$  with extra surfactant, (f) 10 min,  $\times 54K$ , with extra surfactants (duty cycle 60 and output control at 7).

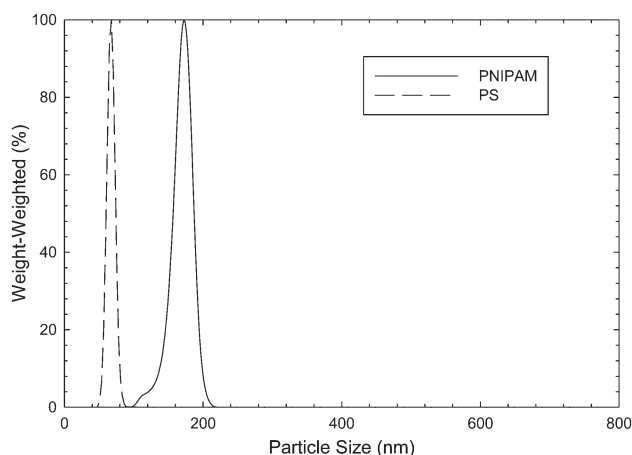


**Figure 8.** PNIPAM and PS latex particle size obtained by CHDF (by weight).

explained by the fact that for a portion of the PNIPAM that was added, there were enough PS particles present in the solution to heterocoagulate, which resulted in full coverage of the PNIPAM-PS “raspberry” particles. However, when more and more PNIPAM particles were added to the blend, the existing PS particles can only cover small portions of the PNIPAM particle surfaces and thus left large areas on the particle surface, which are devoid of any PS particles. In addition, it seems that the PS particles that heterocoagulated with the PNIPAM surface at the beginning of the mixing step did not detach and become redistributed onto other bare PNIPAM particles that were added later. This may indicate that the heterocoagulation of PS particles onto PNIPAM particles is an irreversible process. Therefore, if the number of added PS particles was not high enough to cover all the PNIPAM particle surfaces, both “richly” covered PNIPAM particles and “poorly” covered PNIPAM particles

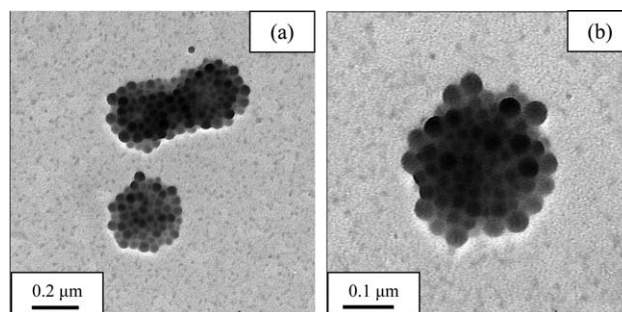


**Figure 10.** TEM micrographs of mixing PNIPAM particles with PS particles after sonification in the presence of extra surfactants (duty cycle 60 and output control at 7).

would exist. These two types of particles cannot equilibrate with each other.

After mixing PS latex with PNIPAM particles at a weight ratio of 2.10 at room temperature, extra surfactant (SDBS) was added to the blended latexes. This latex blend was sonified using a Branson sonifier at a duty cycle at 60 and output power at 7. The extra added surfactant was used to stabilize the PS particles from desorbing off of the PNIPAM surfaces due to the sonification. The TEM micrographs of the particles are shown in Figure 10. The particles still maintained their “raspberry” morphology, which indicates strong interaction between these two types of particles. This experiment further reinforces the hypothesis that during shell formation limited heterocoagulation occurs. This process appears to be irreversible and the interaction between the two kinds of polymers is very strong. This heterocoagulation method may provide a new approach for the encapsulation of hydrophilic particles with hydrophobic material.

By comparing the detailed results obtained in the literature with the results obtained in this current study, it is noted that the

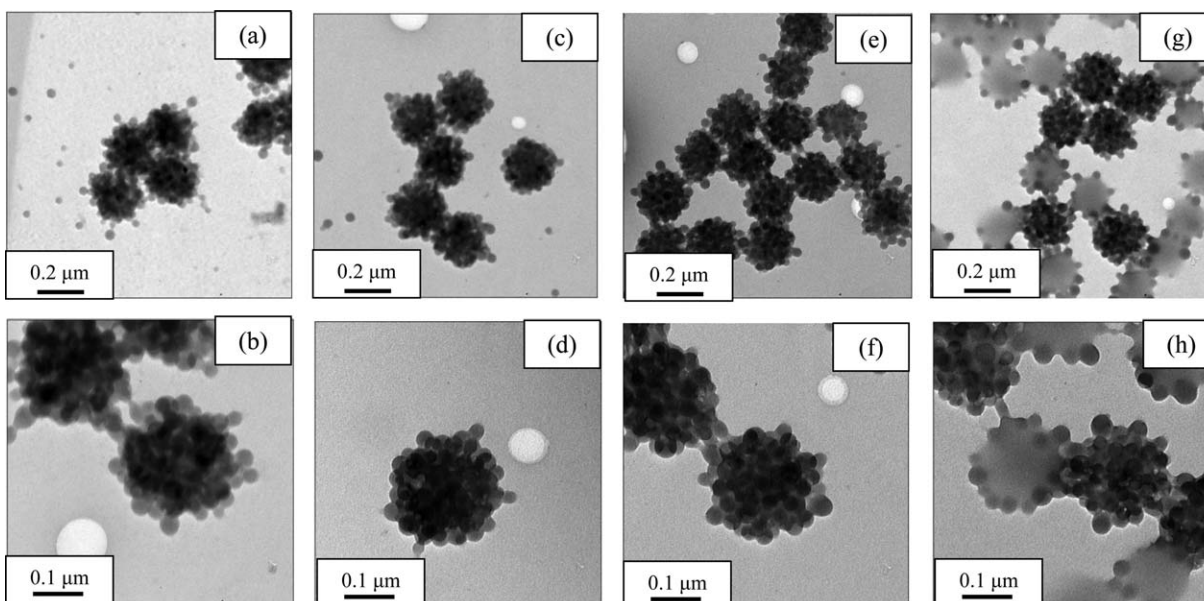


**Figure 9.** TEM micrographs of mixing PNIPAM particle with PS particles (a)  $\times 25K$ , Mix 1; (b)  $\times 54K$ , Mix 1; (c)  $\times 25K$ , Mix 2; (d)  $\times 54K$ , Mix 2; (e)  $\times 25K$ , Mix 3; (f)  $\times 54K$ , Mix 3; (g)  $\times 25K$ , Mix 4; (h)  $\times 54K$ , Mix 4.



mechanism of “raspberry” structure formation can be very different. To clarify these two types of “raspberry” structures, we termed the “raspberry” formation observed in our research as type A and the other type as described in the literature as type B.<sup>5,9</sup> First, these two types of “raspberry” morphologies are different in appearance. In the case of type A particles, each of the “domains” was almost a perfectly smooth half-sphere, which individually resembled small particles. In type B, however, each of the “asperities” was not a perfect half-sphere, but rather a domain as a result of phase separation.<sup>5,9</sup> The author indicated that both phase separation and heterocoagulation may be the reasons for obtaining “raspberry” structured particles. However, during the reaction, small particles were never observed by QELS, which did not favor the heterocoagulation mechanism. The clearly spherical profile of each domain in type A particles and the existence of small particles may indicate that small individual particles may be the precursor of these “domains” and type B particles were more likely formed as a result of phase separation.

Second, the synthesis methods were quite different for type A and type B particles. To form type B particles, many researchers employed copolymerization without using crosslinker during the PNIPAM synthesis. In addition, no emulsifier was used. All of these experimental conditions favor polymerization of styrene within the particle, which then phase separates out of the particle due to the PNIPAM contraction during the drying process. In this research, PNIPAM was crosslinked with MbAA, which helps to reduce the possibility of styrene polymerizing within the particle. Furthermore, in both multistage and semi-batch methods, the core particle PNIPAM formation step was separated from the PS shell formation steps. The use of a slow feed rate with an additional amount of surfactant may help to control the PS particle nucleation in the aqueous phase. Hence, these generated PS particles heterocoagulated with PNIPAM particles.

In addition, unlike the type B particles prepared by both multistage and semi-batch methods, small PS particles were observed in the CHDF particle diameter analysis, which indicated that PS particles were first generated in the aqueous phase. The previously described simple mixing experiment blending PS and PNIPAM particles also further strengthens this view. It was also found that linear PNIPAM may play an important role in stabilizing PS particles during the coagulation process. Therefore, all of our experimental evidence indicates that the mechanism of generating “raspberry” morphology is the result of heterocoagulation, different from type B particles that resulted from phase separation.

What is the force that brings PNIPAM and PS particles together to heterocoagulate? The PNIPAM surface is hydrophobic at 70°C (above its LCST) as is the PS surface. Our previous data<sup>2</sup> has shown that at 70°C, the PNIPAM still contained 20–30% water, making it less hydrophobic (more hydrophilic) than PS. The first report on the interaction between hydrophilic and hydrophobic particles was given by Wesslau et al.<sup>19</sup> where it was claimed that the carboxyl groups are utilized as agglomeration media during the heterocoagulation. In our research, the PS particle surface may not be completely hydrophobic due to the

adsorption of linear PNIPAM onto the PS particle surface. Previous experiments showed that the presence of linear PNIPAM was critical in achieving controlled heterocoagulation.

Second, it was reported that PNIPAM microgels have low surface charge, two orders of magnitude lower than a typical surfactant-free polystyrene latex, due to a much longer chain length.<sup>20</sup> The surface charge of PNIPAM was negative. Three-quarters of the charge resulted from the presence of carboxyl groups, while one-quarter of the charge came from sulfate end-groups. In our case, the PS particles generated during a multistage process may have sulfate end groups present, which originated from KPS initiator. Besides, the SDBS surfactant adsorbs onto the PS particle surface and results in the presence of more sulfonate groups on the surfaces. Therefore, these PS particles surfaces are negatively charged. This may rule out the possibility of the heterocoagulation due to opposite surface charges of the particles.

In addition, efforts were made to calculate the total free energy of all discrete PS particles, all PNIPAM particles, and the total free energy of all “raspberry”-structured PNIPAM/PS core/shell particles. By looking at the difference of these free energies, it would be helpful to understand whether this heterocoagulation is favored from a thermodynamic point view. Unfortunately, the interfacial tension between PS and PNIPAM could not be obtained. Experiments to determine the interfacial tension by measuring the contact angle of PNIPAM solution at different concentrations failed. The highest concentration of PNIPAM solution obtained was 12%. At this concentration, the solution resembled a gel, which possessed a high viscosity. The time needed to reach equilibrium for measuring the contact angle would be too long.

Based on our study of PNIPAM/PS “raspberry” structured particle formation, the following mechanism is suggested (also illustrated in Figure 11). When the PNIPAM polymerization conversion reached 85%, St and surfactant were slowly added. Nucleation of styrene may first occur in the aqueous phase. The existing surfactant serves to stabilize the PS nuclei. When more and more styrene was fed to the system, PS particles grew bigger and bigger. The existing surfactant was not enough to fully stabilize the PS particles. The existence of linear PNIPAM in the aqueous phase assisted the small PS particle stabilization by functioning as a stabilizer. When these particles grew bigger, they became less stabilized. These PS particles interacted with PNIPAM particles, which resulted in heterocoagulation. The existing outer layer of linear PNIPAM increased the compatibility between PS and PNIPAM and also became entangled with the PNIPAM hairy surface when the particles approached one another. Sampling during the reaction showed that this happens at the very early feeding stage. Therefore, after heterocoagulation, the small PS “domains” were likely to continue growing on the surface of PNIPAM. Because of the high instantaneous conversion, the PS domains’ viscosity was too high to coalesce with each other, which resulted in the formation of “raspberry” structured particles. The interaction between PS domains and PNIPAM were determined to be very strong. Thus, heterocoagulation may be an irreversible process.

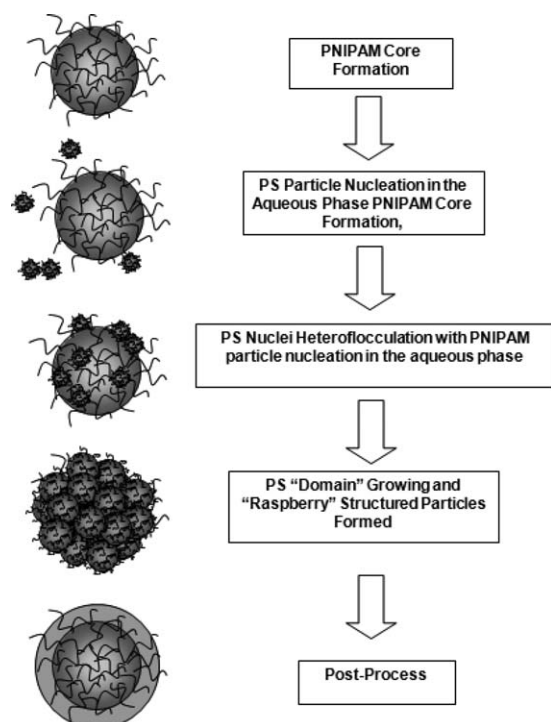


**Figure 11.** Schematic of “raspberry” structured PNIPAM-PS particle formation.

**Application of Heterocoagulation Mechanism: Heterocoagulating PNIPAM with Ludox<sup>®</sup> Nanoparticles to Form Structured Particles.** One example of an application of this heterocoagulation mechanism is to form a hybrid structured particle with a PNIPAM core and a silica shell. The silica used in this experiment was Ludox<sup>®</sup>, which was negatively charged at a pH below 7. Different weight ratios of silica/PNIPAM were

used, and the corresponding TEM micrographs are shown in Figure 12. When the weight ratio of silica to PNIPAM was 3.94, as shown in Figure 12(a,b), it was observed that the PNIPAM particles were fully covered by nanosilica particles. It also appeared that the silica layer was comprised of more than one layer. In addition, individual silica particles still exist between the silica/PNIPAM particles. When the ratio was reduced to 1.88, as shown in Figure 12(c,d), the PNIPAM particles were fully covered by silica particles. There were not many individual silica particles that were observed. By further reducing the weight ratio to 1.08, uniform silica/PNIPAM particles were found, as shown in Figure 12(e,f). Compared with Figure 12(c,d), the PNIPAM particles had a lower surface coverage by the silica at a lower ratio, but were still very uniform. When the weight ratio was reduced to 0.90, as shown in Figure 12(g,h), the density of silica coverage on the PNIPAM surfaces decreased accordingly.

Although several researchers<sup>21,22</sup> have used inverse pickering polymerization to prepare PNIPAM/Silica core-shell particles, the heterocoagulation method has been demonstrated to be a much more convenient approach to produce this type of particles. The heterocoagulation strategy provides several degrees of freedom for controlling morphology and composition of the final materials. First of all, the core materials and shell materials can be two distinct compositions and possess different properties, for example, organic polymers, inorganic polymers, semiconductors, or metals. Second, it permits good control of the dimensions of the core and shell structure, since the core and shell can be prepared individually. For instance, the shell materials can be on the nanoscale, which has great potential in catalytic, magnetic, and electronic fields due to their intrinsic properties. The heterocoagulation strategy may take advantage of new developments in nanotechnology to help design final

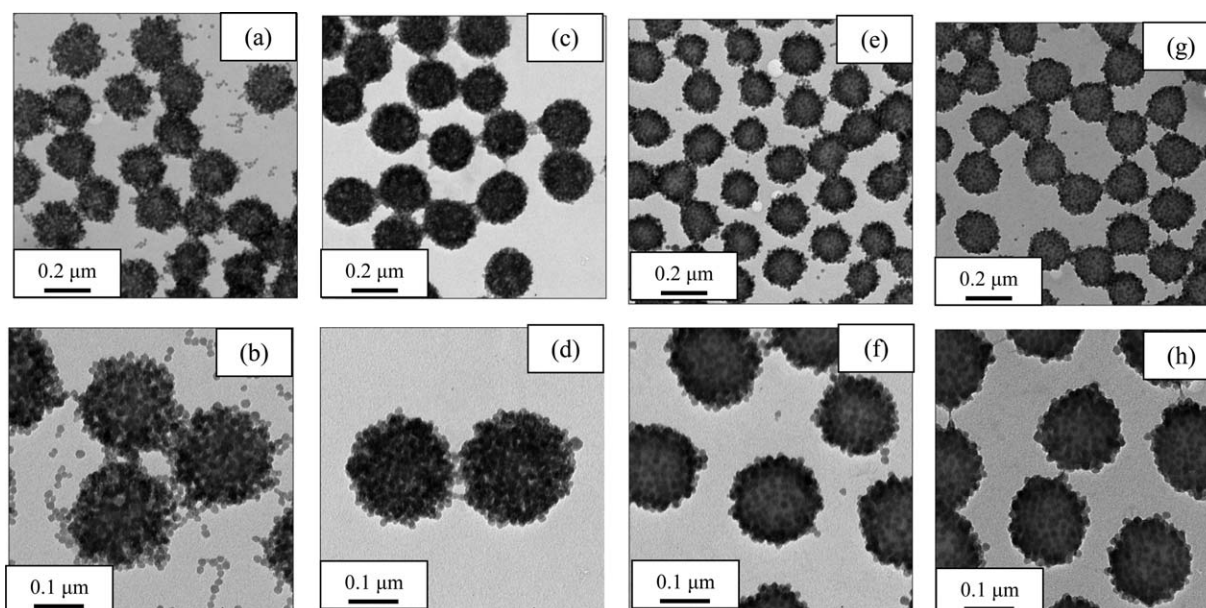


**Figure 12.** TEM micrographs of mixing PNIPAM particle with Ludox<sup>®</sup> nano particles (a)  $\times 25K$ , Mix 1; (b)  $\times 54K$ , Mix 1; (c)  $\times 25K$ , Mix 2; (d)  $\times 54K$ , Mix 2; (e)  $\times 25K$ , Mix 3; (f)  $\times 54K$ , Mix 3; (g)  $\times 25K$ , Mix 4; (h)  $\times 54K$ , Mix 4.

particles for a given application. In addition, these particles may be assembled into a well-defined matrix as well.

## CONCLUSIONS

This study focused on understanding the mechanism of particle formation for PNIPAM/PS core/shell particles. Samples were taken during the polymerization and carefully characterized. It was observed that even at 15-min feed time there were secondary PS particles generated, which were adsorbed onto the PNIPAM particle surfaces. The rough PS surface contours became more gradually obvious as the feeding time of styrene monomer increased. The instantaneous conversion of styrene during the polymerization was quite high, around 95% during the reaction, which helps to explain why the PS domains did not coalesce with each other during the reaction. By varying the feed rate, the obtained “raspberry”-structured particles exhibited different domain diameters and domain numbers, which also supports the hypothesis that polystyrene particles were first generated in the aqueous phase.

Interfacial drop-volume measurements showed that linear PNIPAM exhibited surface activity at temperatures both lower and higher than the LCST. By using semibatch polymerization, it was found that when existing linear PNIPAM were present, smaller PS particles were obtained. These results showed that the linear PNIPAM generated during PNIPAM particle synthesis may function as a stabilizer.

Different ratios of small PS particles were mixed with PNIPAM particles. Similar “raspberry”-structured particles were observed, which further confirmed that PS shell formation is likely to occur by heterocoagulation. This process is likely an irreversible process. The sonification experiments demonstrated that the interaction between the PS domains and PNIPAM particles was very strong. As one application example, the heterocoagulation mechanism was utilized to form a hybrid structured particle with a PNIPAM core and a silica shell.

## REFERENCES

1. Pelton, R. J. *Colloid Interface Sci.*, **2010**, 348, 673.
2. Zhang, L.; Daniels, E. S.; Dimonie, V. L.; Klein, A. *J. Appl. Polym. Sci.*, **2010**, 118, 2502.
3. Taniguchi, T.; Duracher, D.; Delair, T.; Elaissari, A.; Pichot, C. *Colloids Surfaces B Biointerfac.*, **2003**, 29, 53.
4. Wang, P.; He, J.; Wang, P.-N.; Chen, J.-Y. *Photomed. Laser Surg.*, **2010**, 28, 201.
5. Duracher, D.; Sauzedde, F.; Elaissari, A.; Perrin, A.; Pichot, C. *Colloid Polym. Sci.*, **1998**, 276, 219.
6. Ramanan, R. M. K.; Chellamuthu, P.; Tang, L. P.; Nguyen, K. T. *Biotechnol. Prog.*, **2006**, 22, 118.
7. Chen, C. W.; Chen, M. Q.; Serizawa, T.; Akashi, M. *Chem. Commun.*, **1998**, 7, 831.
8. Tkuyama, H.; Yanagawa, K.; Sakohara, S. *Sep. Purif. Technol.*, **2006**, 50, 8.
9. Zhou, G.; Elaissari, A.; Delair, T.; Pichot, C. *Colloid Polym. Sci.*, **1998**, 276, 1131.
10. Lando, J. L.; Oakley, H. T. *J. Colloid. Interface Sci.*, **1967**, 25, 526.
11. Ahmed, S. M.; El-Aasser, M. S.; Pauli, G. H.; Poehlein, G. W.; Vanderhoff, J. W. *J. Colloid Interface Sci.*, **1980**, 73, 388.
12. Harris, B.; Hamielec, A. E.; Marten, L. *Am. Chem. Soc. Symp.*, **1981**, 165, 315.
13. Pelton, R. H.; Chibante, P. *Colloids Surfactants* **1986**, 20, 247.
14. Zhang, J. R.; Pelton, R. *Langmuir*, **1996**, 12, 2611.
15. Zhang, J.; Pelton, R. *Langmuir*, **1999**, 15, 8032.
16. Huggins, H. L. *J. Am. Chem. Soc.*, **1942**, 64, 2716.
17. Kraemer, E. O. *Ind. Eng. Chem.*, **1938**, 30, 1200.
18. Zhu, P. W.; Napper, D. H.; *Colloids Surf. A Physicochem. Eng. Aspects*, **1995**, 98, 93.
19. Keppler, H. G.; Wesslau, H.; Sabenow, J. S. *Angew. Macromol. Chem.*, **1968**, 2, 1.
20. McPhee, W.; Tam, K. C.; Pelton, R. *J. Colloid Interface Sci.*, **1993**, 156, 24.
21. Duan, L. M.; Chen, M.; Zhou, S.; Wu, L. *Langmuir*, **2009**, 25, 3467.
22. Cejkova, J.; Hanus, J.; Stepanek, F. *J. Colloid Interface Sci.*, **2010**, 346, 352.